A Monolithic CMOS Microhotplate-Based Gas Sensor System

Muhammad Y. Afridi, *Member, IEEE*, John S. Suehle, *Senior Member, IEEE*, Mona E. Zaghloul, *Fellow, IEEE*, David W. Berning, Allen R. Hefner, *Fellow, IEEE*, Richard E. Cavicchi, Steve Semancik, Christopher B. Montgomery, and Charles J. Taylor

***Abstract*—A monolithic CMOS microhotplate-based conductance-type gas sensor system is described. A bulk micromachining technique is used to create suspended microhotplate structures that serve as sensing film platforms. The thermal properties of the microhotplates include a 1-ms thermal time constant and a 10 °C/mW thermal efficiency. The polysilicon used for the microhotplate heater exhibits a temperature coefficient of resistance of 1.067×10^{-3}/°C. Tin(IV) oxide and titanium(IV) oxide (SnO_2, TiO_2) sensing films are grown over postpatterned gold sensing electrodes on the microhotplate using low-pressure chemical vapor deposition (LPCVD). An array of microhotplate gas sensors with different sensing film properties is fabricated by using a different temperature for each microhotplate during the LPCVD film growth process. Interface circuits are designed and implemented monolithically with the array of microhotplate gas sensors. Bipolar transistors are found to be a good choice for the heater drivers, and MOSFET switches are suitable for addressing the sensing films. An on-chip operational amplifier improves the signal-to-noise ratio and produces a robust output signal. Isothermal responses demonstrate the ability of the sensors to detect different gas molecules over a wide range of concentrations including detection below 100 nanomoles/mole.**

I. Introduction

CHEMICAL microsensors represent one important application for microelectromechanical systems (MEMS) technology. Microhotplate devices belong to the MEMS family and can be fabricated in commercial CMOS technology using micromachining techniques [1]. Thermally isolated microhotplate structures can be utilized for conductance-type gas sensing [2] or as microscopic infrared sources [3]. The CMOS compatible process realizes a class of devices that are based on thermo-electromechanical effects and are compatible with existing very-large-scale-integration (VLSI) circuit design techniques [4]–[6]. In this paper, a monolithic integration of a gas sensor system based on CMOS-compatible microhotplate technology is presented. There are numerous applications available for the low-cost monolithic integrated gas sensors. For example, these sensors could be used to detect the freshness of food products, the leakage of toxins in chemical manufacturing facilities, or dangerous chemical agents in public places.

Conductance-type gas sensors often need elevated platform temperatures to activate the sensing mechanism. The microhotplate is a perfect platform for such devices because of its small size and ease of fabrication using standard commercial CMOS technology [1]. Such micromachined structures offer many potential advantages for sensing applications including low power consumption, low fabrication cost, high quality, and reliability. Furthermore, the microhotplate's high thermal efficiency, low thermal time constant, and small size facilitate building arrays of sensors needed for classification of gases in complex gas sensing environments. The CMOS-compatible process used for the gas sensors in this work also enables the monolithic integration of the sensors with electronic circuits.

Array implementation of the micro-gas-sensor system demands an efficient way to select and measure data from each array element. CMOS technology enables monolithic integration of microhotplate and interface circuitry to comprise a conductance-type gas sensor system [7]. In Sections II–IV, the microhotplate sensor element and interface circuitry are described and characterized. Performance evaluation of the gas sensor system is also given.

II. Microhotplate Gas Sensor Element Structure

Fabricated with micromachining technology, the microhotplate [1] is a suspended structure, which contains a heating element. For example, the microhotplate can be fabricated using a standard commercial CMOS process and can use a polysilicon layer for a resistor-heating element. As silicon is a good heat conductor, it must be removed from underneath the microhotplate to achieve high thermal efficiency. The localized removal of silicon from desired places is accomplished by using bulk micromachining techniques [8]. Xenon difluoride (XeF_2) can be used as a silicon etchant in this post-CMOS process. The microhotplate often incorporates an aluminum heat-spreading layer to achieve uniform temperature distribution over its surface. The small size of the microhotplate allows it to have a low thermal time constant.

A. Microhotplate-Based Gas Sensor Element Design and Fabrication

The metal oxide-based thin-film gas sensors typically require elevated temperatures (200 °C to 400 °C) to detect gas species

Manuscript received November 19, 2002. The associate editor coordinating the review of this paper and approving it for publication was Prof. Gert Cauwenberghs.

M. Y. Afridi, J. S. Suehle, D. W. Berning, and A. R. Hefner are with the Semiconductor Electronics Division, National Institute of Standards and Technology (NIST), Gaithersburg, MD 20899 USA (e-mail: afridi@nist.gov).

M. E. Zaghloul is with the Electrical and Computer Engineering Department, The George Washington University, Washington, DC 20052 USA.

R. E. Cavicchi, S. Semancik, and C. B. Montgomery are with the Process Measurements Division, National Institute of Standards and Technology (NIST), Gaithersburg, MD 20899 USA.

C. J. Taylor is with the Seaver Chemistry Laboratory, Pomona College, Claremont, CA 91711 USA.

Digital Object Identifier 10.1109/JSEN.2002.807780

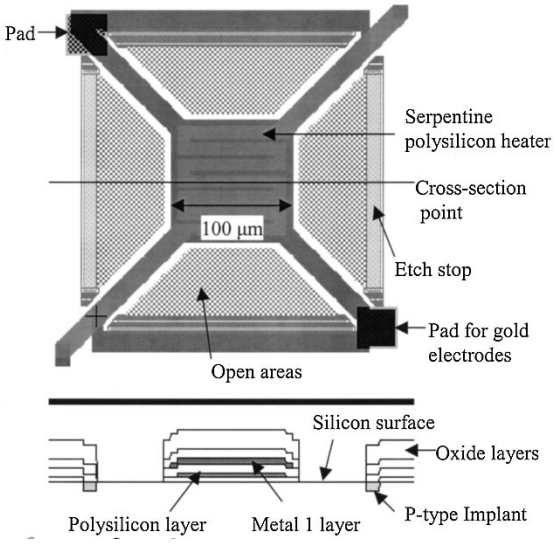

Fig. 1. Top and cross-sectional views of the microhotplate layout design.

[9]. The high thermal efficiency and low thermal time constant (typically 1 ms) suggest using the microhotplate to implement a metal oxide-based gas sensing system. Their small size makes it practical to implement an array of gas sensors by replicating the microhotplate design.

In this work, a four-by-one array of gas sensor elements is combined with integrated electronics to form a monolithic gas sensing system. However, the design strategy presented can be used for an n-by-m matrix of gas-sensing elements. The interface design of the gas sensor system is described in Section III. This section describes the design and fabrication of the microhotplate-based, conductance-type, gas-sensing element.

The microhotplate is designed using a layout editor. Fig. 1 shows the CMOS-compatible microhotplate layout design and a cross-sectional view. This view does not include any postprocessing attributes. The design has four trapezoidal open areas that facilitate postprocess etching of exposed silicon to create a pit, above which the microhotplate is suspended. The serpentine polysilicon shape defines the 2-kΩ microhotplate heating element. The design criterion for the microheating element includes the operating voltages and currents for the microheating resistor. The value for the current is chosen such that the heating material does not suffer any problems associated with excessive joule heating. The operating voltage is chosen to avoid oxide breakdown across the intradielectric layers. The aluminum layer (metal 1) of the CMOS process is used as a heat spreader. The two pads shown in the figure are used for making connections to the gold electrodes which are postprocessed onto the suspended region. Their use is described later in the paper. The outer perimeter of the microhotplate design has a P-type implant that is used as an etch stop.

The mask layers that are used to provide openings to the exposed silicon surface are listed in Table I. Superposition of these mask layers results in the removal of the four dielectric layers of the CMOS process. The required superposition of these masks violates several CMOS design rules. However, these violations do not jeopardize the normal processing steps required for CMOS circuit fabrication. These open areas allow silicon etchant to remove the silicon from desired areas in the postprocess steps described below. To use the microhotplate as a platform for gas-sensing applications, a mask is designed to pattern gold electrodes over the microhotplate structure as a postprocessing step. This mask creates sensing electrodes that connect to the pads indicated in Fig. 1. Metal–oxide sensing films are grown over these sensing electrodes covering the entire suspended active area of the microhotplate to complete the gas sensor elements.

Fig. 2 shows a flow chart of the steps required to fabricate the micro-gas-sensor system. In this work, a 1.5-μm CMOS technology is used to implement the design. Once the chip is received from the CMOS foundry, the postprocessing steps begin.

Gold electrodes are fabricated on the top of the microhotplate by coating the CMOS chip with 200 Å of chromium and 4000 Å of gold. The chromium is used as an adhesion layer for gold because gold does not adhere well to the SiO_2 dielectric. Before the sputter deposition of the chromium and gold on the chip, the chip is *in situ* ion-beam cleaned with argon to remove aluminum oxide from the pads (Fig. 1) that make contact to the postprocessed gold electrodes.

After the chromium and gold deposition, the chip is coated with photoresist for patterning the gold electrodes. Contact mask photolithography is used to pattern gold electrodes. The chip is developed in photoresist developer followed by gold and chromium etching processes. The gold etchant is prepared using 80 g of KI and 20 g of I_2 in 800 ml of H_2O. The mixture is stirred for 1 h at room temperature before use. Four thousand ångströms of gold is removed in 2 min and 30 s at room temperature with this gold etchant. The chip is dipped in a standard chromium etchant for 3 s to remove 200 Å of chromium. A xenon difluoride (XeF_2) etch is then performed on the chip to create the suspended microhotplate structures, as shown in Fig. 3(b). The chip is mounted in a 40-pin dip package and wire bonded.

In order to make a direct comparison between the sensing characteristics of two different metal–oxide thin films, tin(IV) oxide and titanium(IV) oxide films are grown over postpatterned gold sensing electrodes by low-pressure chemical vapor deposition (LPCVD) using tin(IV) nitrate and titanium(IV) isopropoxide as the precursors [10]. The precursor temperatures are 25 °C and 28 °C for the tin(IV) nitrate and titanium(IV) isopropoxide, respectively. Argon is used as the carrier gas with a flow rate of 10 sccm. The reactor pressure is 66.661 Pa (0.5 torr). Sensing films are deposited at 250 °C and 300 °C for SnO_2 and TiO_2 films, respectively. Deposition times are 15 min. Fig. 4 shows the block diagram for the CVD process.

Fig. 3 shows a postprocessed microhotplate gas-sensing element. Fig. 3(a) shows a cross-sectional sketch and Fig. 3(b) is an SEM micrograph. The two gold electrodes can be seen in the SEM micrograph, and the sensing films are grown over the entire heated surface of the microhotplate. The sensing films thus straddle the area between the gold electrodes, and this portion of the film determines the response of the sensor.

B. Microhotplate Characterization

Microhotplate gas sensor elements are characterized using both electrical and infrared thermal imaging methods. The mi-

TABLE I
MASKS REQUIRED FOR CREATING OPEN AREAS TO FACILITATE BULK MICROMACHINING

Mask name	CIF ID
Active	CAA
Active contact	CCA
Via	CVA
Overglass	COG

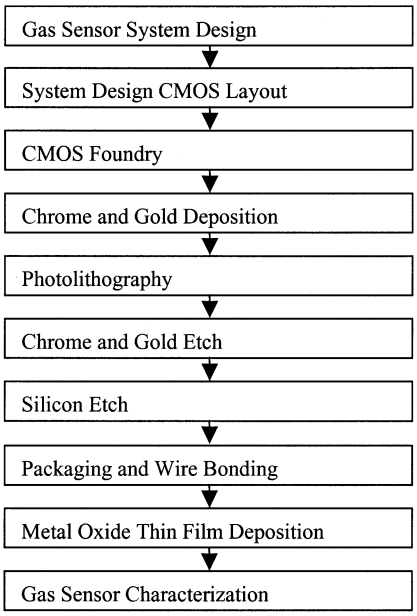

Fig. 2. Flowchart of gas sensor system fabrication and testing.

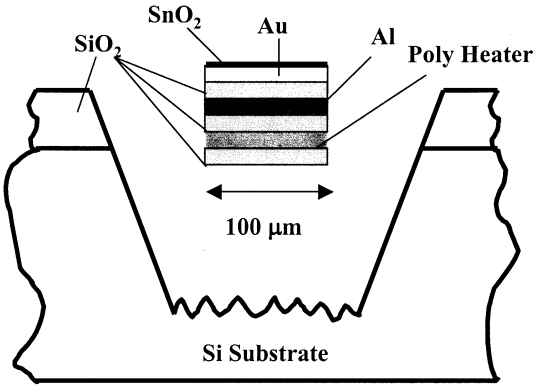

(a)

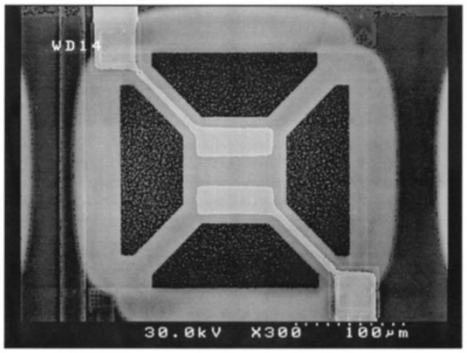

(b)

Fig. 3. Microhotplate. (a) Cross section of layer structure. (b) SEM micrograph of the suspended microhotplate structure with the postprocessed gold gas-sensing electrodes.

crohotplate polysilicon heater temperature coefficient of resistance (TCR) is measured electrically by heating the device externally with a temperature-controlled hotplate and measuring the resistance of the polysilicon heater. Temperature measurements are taken at the top of the chip ceramic package with a temperature probe. To avoid additional joule heating due to the microhotplate heating element, a small constant dc current (100 μA) is forced through the polysilicon heater, and voltage measurements are taken across the heater. The temperature of the hotplate is increased in 20° steps to 250 °C, and voltage measurements are made for each temperature step once thermal equilibrium is reached. Fig. 5 shows the experimental values of these measurements, as well as a linear fit to this data.

The TCR value for polysilicon used in the 1.5-μm CMOS technology is obtained using the equation

$$\frac{\Delta R}{R_0} = \alpha \Delta T \tag{1}$$

where ΔR is the change in resistance, ΔT is the change in temperature, and R_0 is the resistance of polysilicon resistor at 25 °C. The microhotplate polysilicon resistor characterized in Fig. 5 exhibits a positive TCR of $\alpha = 1.067 \times 10^{-3}/°\mathrm{C}$.

The thermal efficiency of the microhotplate is found by electrically heating the microhotplate polysilicon resistor with known power levels and measuring the resistance values. The resistances are then correlated to the corresponding temperatures using the TCR value of the polysilicon. The microhotplate characterized in Fig. 5 has a thermal efficiency of 10 °C/mW.

A high-speed thermal imaging system [11], [12] is used to investigate the dynamic thermal behavior of microhotplate devices of several different technologies and structures. This system generates a sequence of thermal contour map images and is used to measure heating dynamics. It uses an infrared detector that is configured to measure fast transient waveforms of a single point on the sample. The test sample is moved under the detector in a step-and-repeat fashion by motorized translation stages, and recorded waveforms are assembled into a sequence of images.

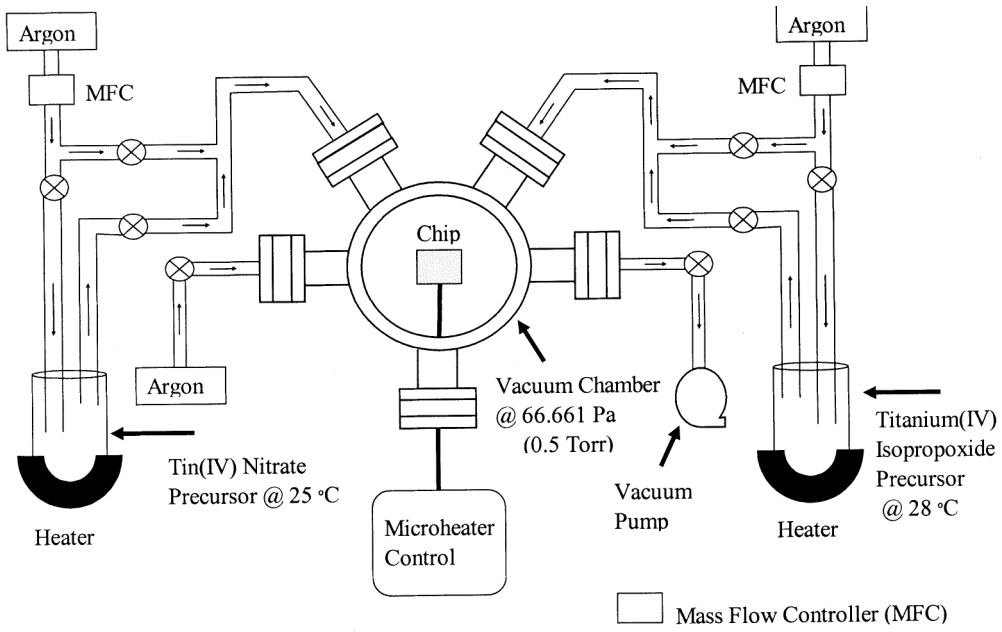

Fig. 4. LPCVD setup.

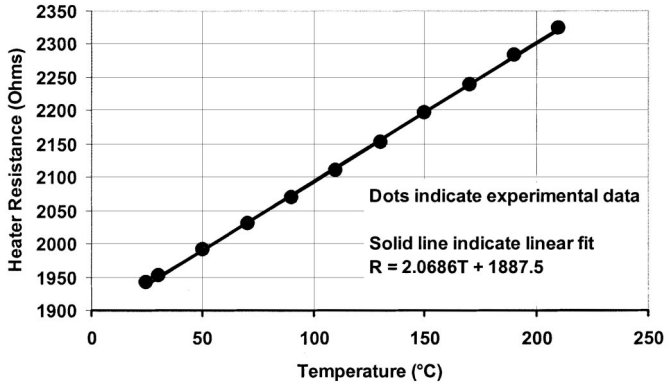

Fig. 5. Polysilicon TCR measurement data.

Fig. 6 shows thermal images with associated heating and cooling responses for the 1.5-μm CMOS-technology-based microhotplate. A relatively long (2 ms) heating pulse is used, and the microhotplate temperature is observed to approach a steady-state condition before the heating pulse is removed. In Fig. 6(a), a temperature contour map is shown for the maximum temperature point, and in Fig. 6(b) a map is shown 1.5 ms after power is removed and the microhotplate has substantially cooled from its maximum temperature. In the image associated with Fig. 6(b), the four suspending legs of the microhotplate retain a small amount of heat and are visible.

The infrared imaging system has been employed to determine optimum design features of the microhotplate structures. Some of the desirable design features include the use of a heat-spreading layer to obtain uniform surface temperature and the use of thin dielectric layers for fast thermal response [12].

III. Integrated Gas Sensor System

Adsorption of gas species onto the surface of a metal–oxide–semiconductor can produce a substantial change in its electrical resistance. This change in resistance results from the loss or gain of surface electrons as a result of adsorbed oxygen reacting with other types of gas molecules. Conductometric metal–oxide gas sensors are based on this phenomenon. Since the change in electrical resistance in the sensing metal–oxide film is caused by a surface reaction, it is desirable to make the sensing film thinner with a substantial surface area for an optimum response to a gas.

It is observed that metal–oxide gas sensors often respond to a wide range of gas species and are therefore typically only partially selective. However, grain size in the metal–oxide film does have an effect on the relative resistivity of the film to different gas species. Grain size of a particular metal–oxide film is affected by the growth temperature. Individual microhotplate heaters can be used to control this temperature during the film growth process. An array of these micro-gas-sensors with different film structures (e.g., different grain sizes) can be used to achieve different response signatures for different gases.

It is desirable to combine an array of unique gas sensor elements (different material types or microstructures) with integrated electronics that can address individual elements and output a signal that can be analyzed to determine gas classification. An efficient interface circuit is needed to measure the response of each array element. To keep the power consumption of the gas sensor system low, an efficient heater power-switching scheme is also needed. Section III-A describes such an interface system developed in this work.

A. Interface Design

In this section, an interface circuit for automatic sensor selection and conductance measurement is described. The interface design has both analog and digital circuitry, as shown in Fig. 7. The analog circuit is comprised of an operational amplifier, and the digital circuitry has two decoders/multiplexers. To measure the conductance of the metal–oxide

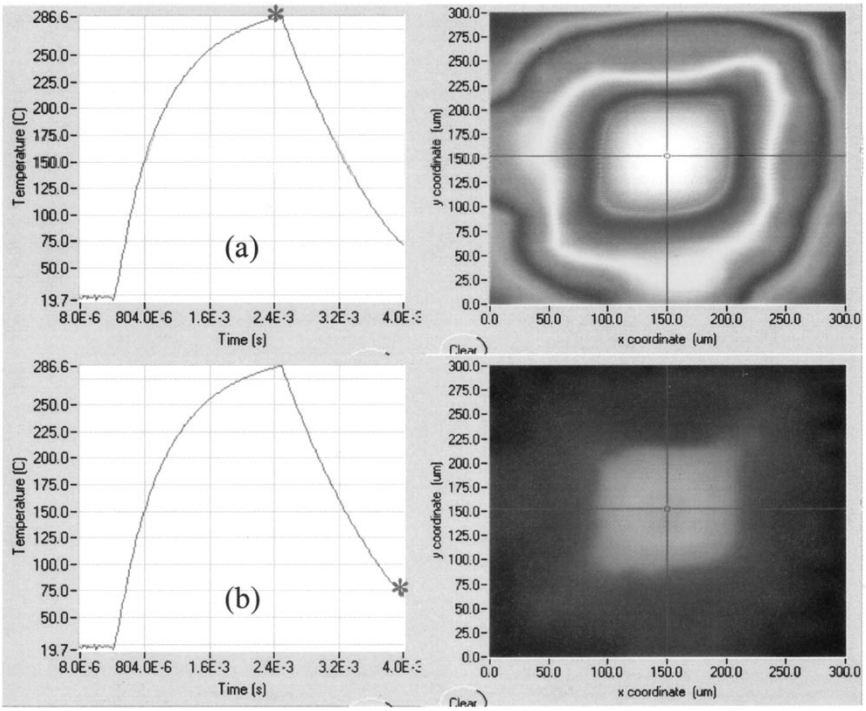

Fig. 6. Thermal images of 1.5-μm CMOS-based microhotplate (a) at maximum temperature and (b) after partially cooled.

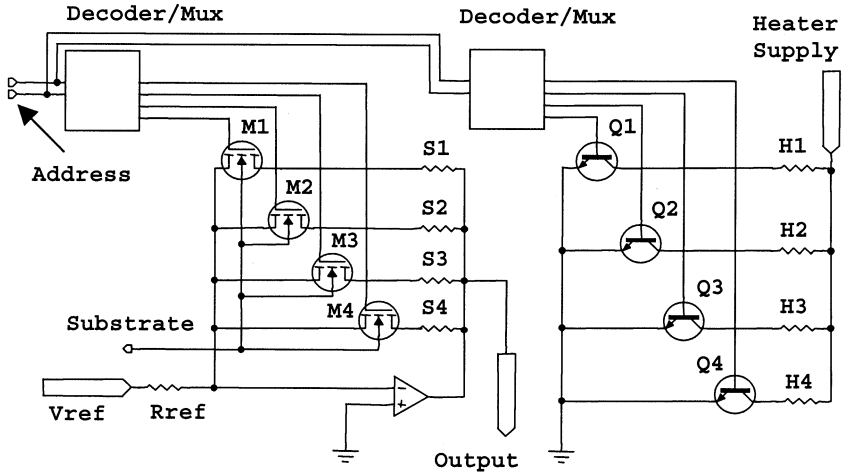

Fig. 7. Interface circuit schematic.

sensing film, an inverting operational amplifier configuration is used, where the sensing film is in the feedback loop of the amplifier. The digital portion of the interface circuit contains both a selectable sensor array $(S1, S2, \ldots, S4)$ and a selectable heater array $(H1, H2, \ldots, H4)$. The address lines for the two decoders/multiplexers are tied together as shown in Fig. 7. One decoder/multiplexer activates the MOSFET sensor selection switches $(M1, M2, \ldots, M4)$, while the other activates the bipolar heater switches $(Q1, Q2, \ldots, Q4)$. Bipolar junction transistors (BJTs) are used for heater switching because of the higher voltage and current requirements. MOSFET switches are used for sensor array switching because of their small dc offset. Only one heater–sensor pair is activated at one time.

The on-chip operational amplifier is designed and configured to measure the conductance of a selected sensing film within the gas sensor array. A circuit schematic of the operational amplifier is shown in Fig. 8. Due to the very large open-loop gain and high input resistance, the closed-loop gain of the inverting amplifier depends only on Rref (external to the chip, Fig. 7) and the sensor's resistance (e.g., S1). Since Rref is fixed, the output of the amplifier reflects the conductance of the selected sensor element. The resistances of the MOSFET switches are generally three orders of magnitude less than the resistances of the sensing films and thus can be neglected. The advantage of this scheme is that only one operational amplifier and two decoders are needed to measure the conductance changes of all of the elements of the gas array. Furthermore, variations in Vref, Rref, and amplifier offset and gain will track for all sensing elements.

The digital portion of the micro-gas-sensor system, comprised of the 2-b decoders/multiplexers, is designed and

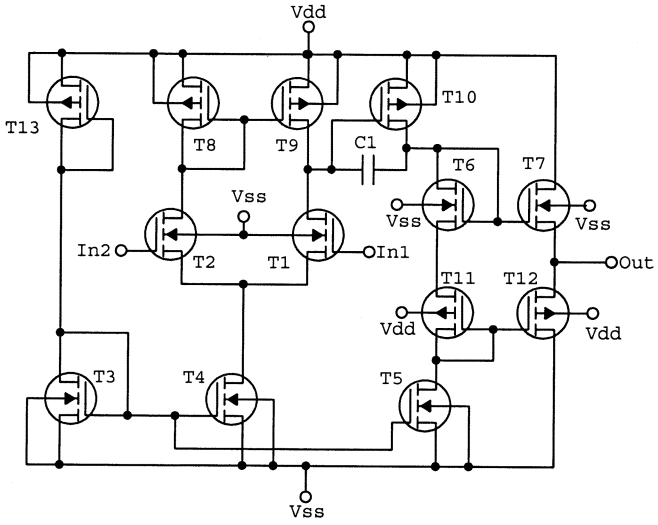

Fig. 8. Operational amplifier schematic.

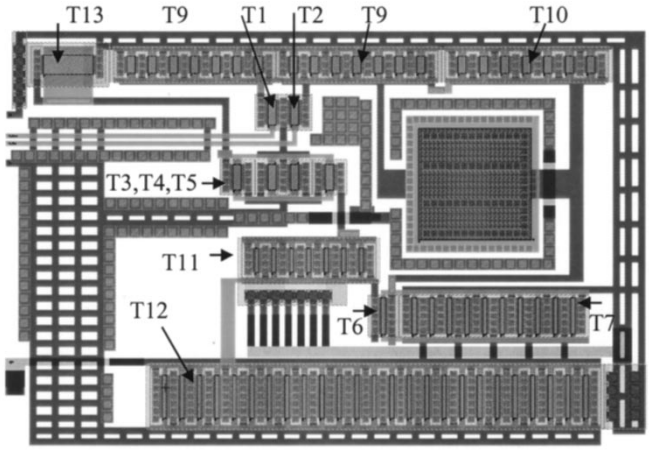

Fig. 9. Operational amplifier layout (410 μm$\times$ 275 μm).

TABLE II
TRANSISTOR SIZES

Reference designator	Length(μm)	Width (μm)	Channel Type	W/L
T1	5	15	N	3
T2	5	15	N	3
T3	5	15	N	3
T5	5	15	N	3
T4	5	30	N	6
T6	2	15	N	7.5
T7	2	150	N	75
T8	5	70	P	14
T9	5	70	P	14
T10	5	70	P	14
T11	2	70	P	35
T12	2	700	P	350
T13	30	5	P	0.166

implemented using a standard CMOS gate cell library. The layout for the 2-b decoders/multiplexers is generated automatically by the layout program. Two separate decoders are used because of the different drive requirements of the MOSFET and bipolar switches. The MOSFET switch transistor layout is done manually to insure low ON-resistance.

The analog part of the interface circuit, which includes the operational amplifier, is designed using a typical three-stage configuration scheme [13]. This scheme includes the input differential stage, a gain stage, and the output buffer stage. The layout for the operational amplifier is also done manually to optimize device matching and performance. The custom layout of this operational amplifier is shown in Fig. 9. Table II lists the transistor sizes for this amplifier design.

The operational amplifier is operated from a single power supply of 5 V and a 2.5-V bias is applied to the noninverting input to obtain the maximum output dynamic range. In the operational amplifier, transistors T1 and T2 (Fig. 8) are the input transistors of the differential stage. T10 provides most of the gain of the amplifier. T7 and T12 serve as the output buffer stage. All other transistors act as current source loads or current references.

Fig. 10 shows a micrograph of the integrated gas sensor system. Some additional test structures and an additional operational amplifier are included for characterization purposes.

B. System Component Characterization

Fig. 11 shows the measured transfer characteristics of one of the BJT switches. The collector breakdown voltage exceeds 30 V. The current gain is 50 at a collector current of 5 mA and 1 V collector to emitter. This operating point is sufficient to elevate the microhotplate surface temperature to 500 °C. BJTs were fabricated using the P-base layer provided by the CMOS process.

To characterize the operational amplifier test structure, it is configured as an inverting amplifier with a gain of five, set by external resistors for this measurement. The input is 0.5 V peak to peak, and the measured output is 2 V peak to peak with slight clipping. The amplifier is overdriven to observe its dynamic range. The speed of the amplifier is sufficient with this gain to reproduce a square wave of 100 kHz.

IV. GAS SENSOR SYSTEM CHARACTERIZATION AND RESULTS

Performance characteristics for the gas sensor system are described for different gas species and concentrations. For all of the measurements made, the microhotplate temperature is kept constant at 250 °C. Measurements include the responses from both SnO_2 and TiO_2 sensing films. The first part of this section describes the test system while the second part of this section presents measurement results and discussion.

A. Description of the Test System

Fig. 12 shows the electrical measurement test circuit used for the gas sensor system. A sinusoid of 1 kHz is used as a reference signal, and the rms value of the operational amplifier output is recorded with an ac voltmeter. The capacitive coupling of the reference sinusoidal signal prevents dc drift and offset problems in the measurements. The operational amplifier is powered with a single supply of 5 V. An appropriate dc bias is applied to the noninverting amplifier input to achieve symmetric clipping for maximum dynamic range. Rref is chosen to obtain the maximum output voltage without clipping under the various gas sensing conditions. An appropriate address is applied to the MUX to select the desired gas-sensing element.

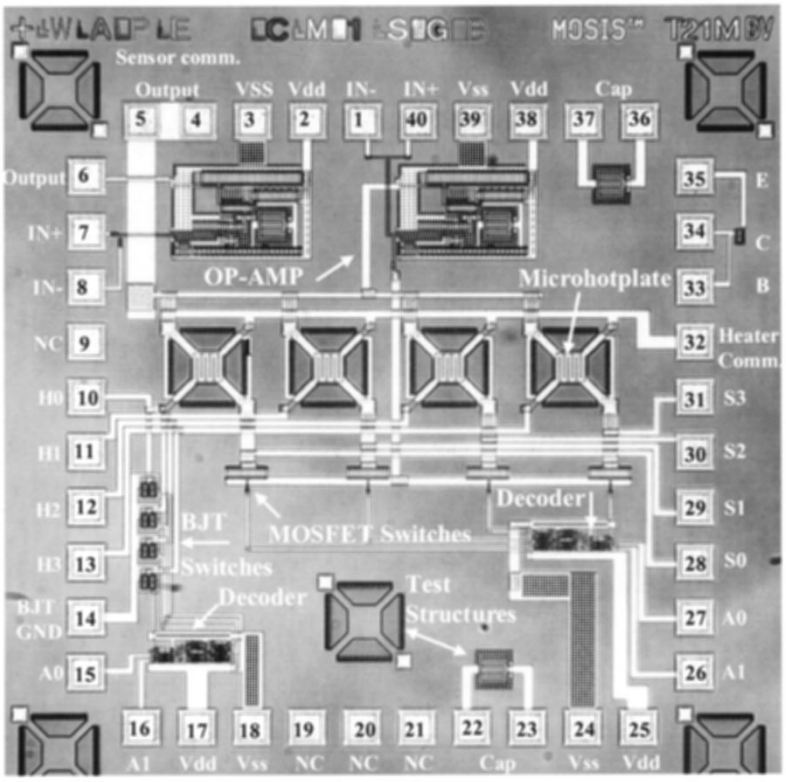

Fig. 10. Micrograph of the integrated gas sensor system.

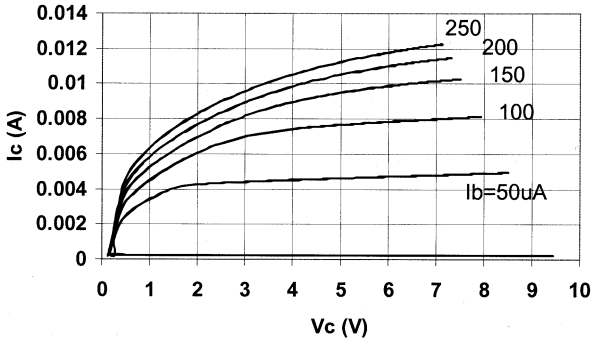

Fig. 11. BJT *I–V* curves.

An automated gas flow system is used to expose the gas sensors to a known concentration of one test gas at a time. This setup includes precision flow controllers and ON/OFF valves for the test gases. The valves are open or closed under the direction of a computer program. The gases tested include hydrogen, acetone, methanol, and carbon monoxide. The gas sensors are subjected to these gases in calibrated concentrations for 200 s and then purged with dry air for 300 s. Two cycles of five different gas concentrations are obtained for each test gas, and the results are discussed below.

Fig. 13 shows the functional block diagram of the gas sensor characterization setup that is used in this work. The test gases are diluted with the dry air to achieve the desired low concentrations. The mass flow controllers (MFCs) are controlled by a computer program to select the desired concentration. Just one test gas is on at any single time during this gas sensor characterization. A computer-controlled switch directs the test gas either to the exhaust or to the test chamber. The chip output and control signals are used to gather data from the gas sensor system.

B. Measurement Results and Discussion

Fig. 14 shows the responses of both SnO_2 and TiO_2 sensing films to various concentrations of the test gases. Fig. 14(a) shows the SnO_2 sensing film response to hydrogen gas. Two cycles of five different concentration levels of the hydrogen gas are shown. A large signal is achieved even with the 6 micromoles/mole gas concentration. This result can be compared with Fig. 14(b) that shows hydrogen on TiO_2 sensing film. The response of TiO_2 to hydrogen is about twice as strong as the response of SnO_2 to hydrogen. The apparent time constant of adsorption and desorption of hydrogen is similar for both sensing films.

For the carbon monoxide test gas, the SnO_2 film shows a good response to 6 micromoles/mole gas concentration, as shown in Fig. 14(c). However, the TiO_2 film response is saturated with only 6 micromoles/mole of carbon monoxide gas. Therefore, the gas concentration is lowered by a factor of 60 as shown in Fig. 14(d), where the carbon monoxide gas concentration starting point is 100 nanomoles/mole. The apparent time constant of adsorption and desorption of carbon monoxide is longer for the TiO_2 sensing film.

Fig. 14(e) shows the SnO_2 film response to methanol. It is obvious from the graph that, for methanol, recovery of the SnO_2 film requires much more time as compared to hydrogen and carbon monoxide. Fig. 14(f) shows the TiO_2 film response to methanol. The TiO_2 response is much stronger than SnO_2, and similarly the TiO_2 film required a longer recovery time.

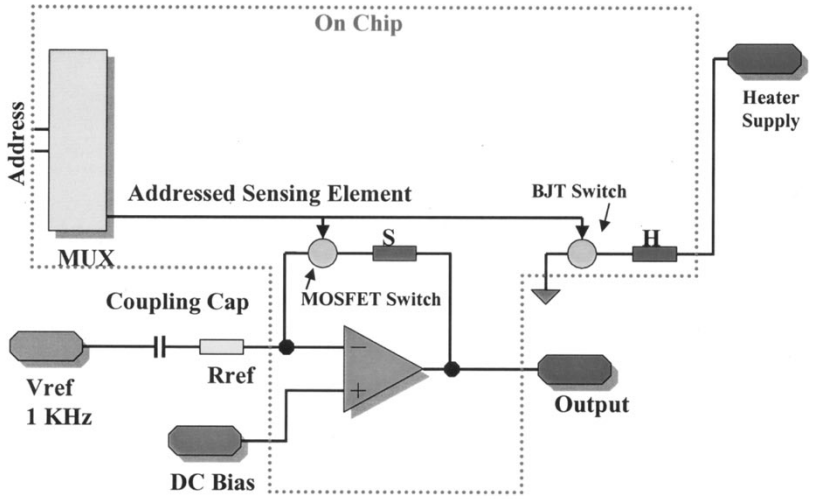

Fig. 12. Electrical measurement test circuit.

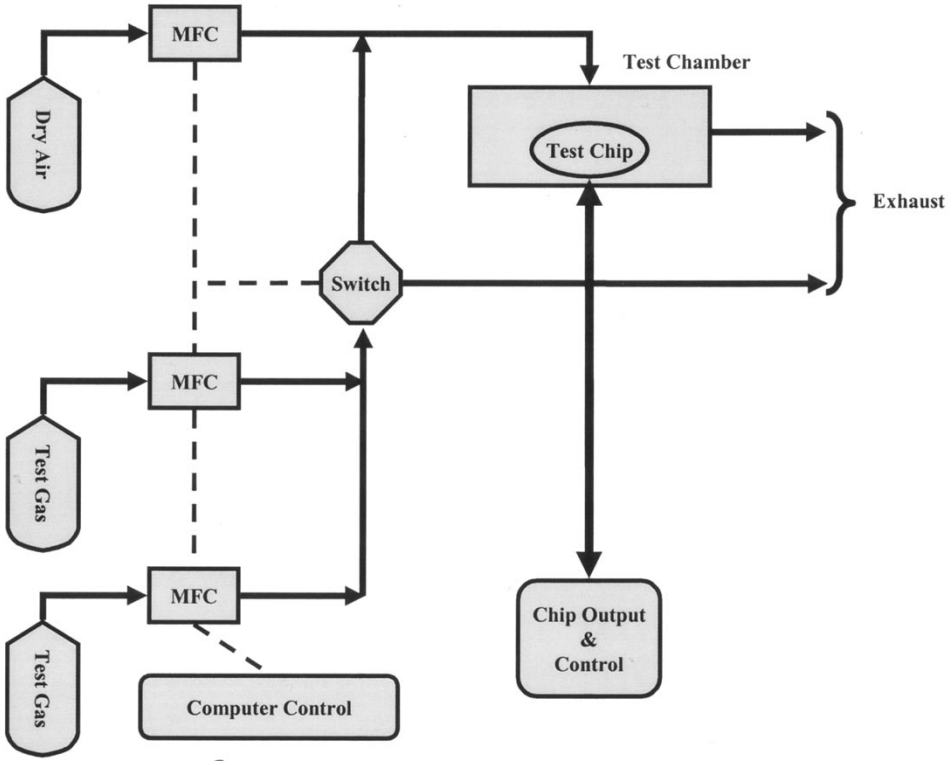

Fig. 13. Block diagram of the gas sensor characterization setup.

Fig. 15 depicts the gas concentration versus the ΔV output voltage. It is observed from this graph that these metal–oxide films are more sensitive at concentration levels less than 12 μmoles/mole. Titanium oxide shows a very high sensitivity to carbon monoxide. The graph labeled methanol on titanium oxide shows a decrease in the ΔV output voltage because methanol requires more time for recovery, as can be seen in Fig. 14(f).

Fig. 16 shows a comparison of gas sensor response to CO. The gas sensor response of this work is compared with a commercially available gas sensor and the response reported by Barrettino [14]. For comparison, the data are manipulated to get the percentage change in the sensing parameter of the gas sensor. Neither the commercial gas sensor nor the data shown by Barrettino address CO gas concentrations below 10 micromoles/mole, whereas the sensor response of this work to CO gas concentration is shown to be as low as 100 nanomoles/mole.

The SnO_2 and TiO_2 thin-film-based sensors are very sensitive to methanol and acetone. High concentration saturates the sensor response. The adsorption and desorption time for each gas species is different.

V. Conclusion

In this paper, we have presented a monolithic implementation of a CMOS compatible microhotplate-based conductance-type gas sensor system. An efficient interface design is presented for an array of gas sensor system configuration. It is found that

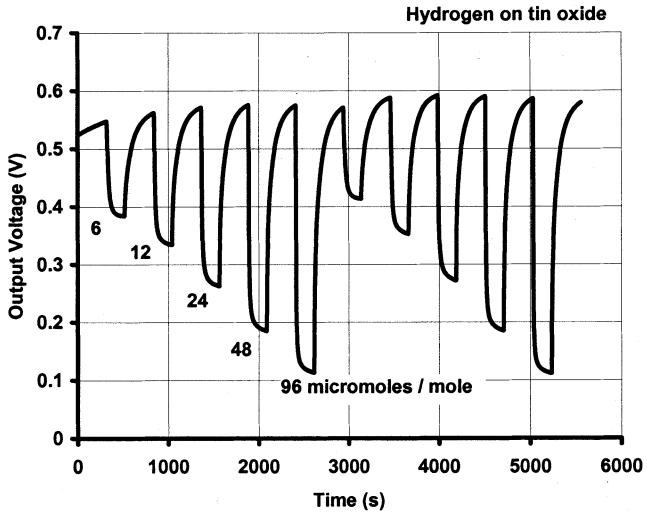

(a)

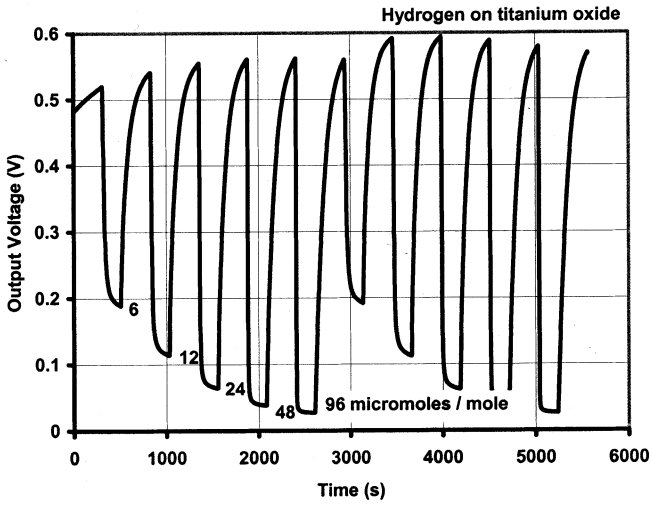

(b)

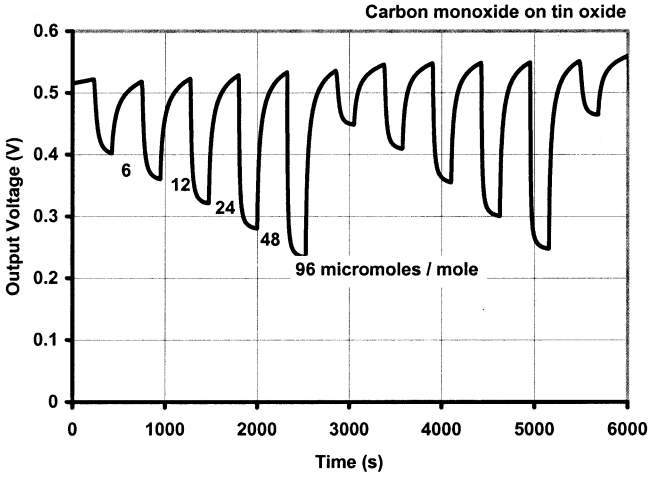

(c)

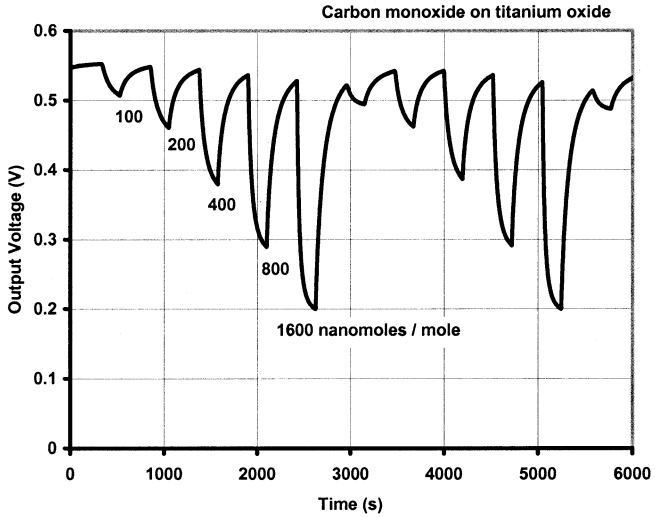

(d)

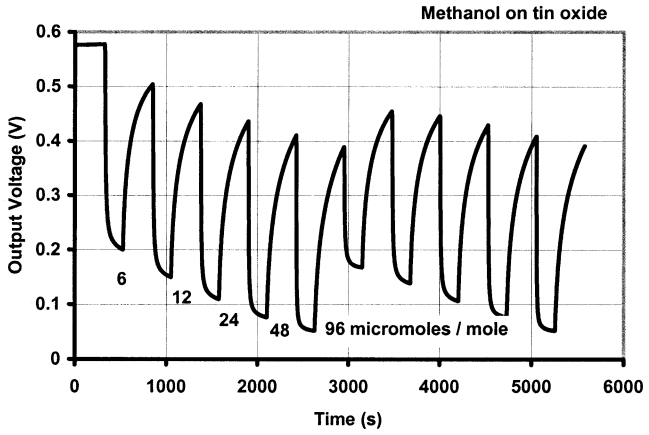

(e)

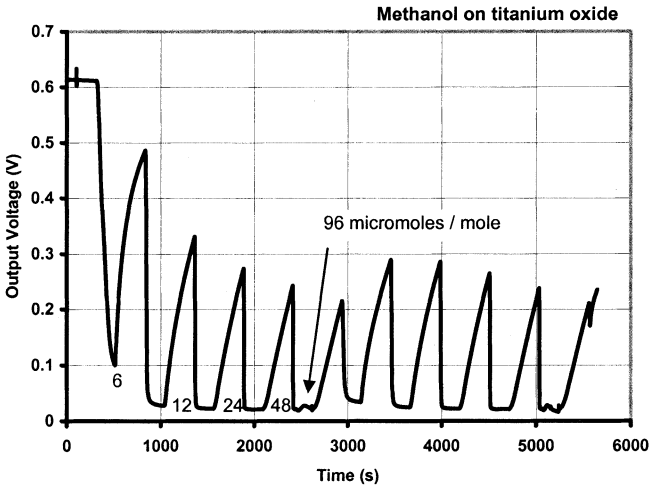

(f)

Fig. 14. Responses of both SnO_2 and TiO_2 sensing films to various test gas concentrations. (a) H_2 on SnO_2. (b) H_2 on TiO_2. (c) CO on SnO_2. (d) CO on TiO_2. (e) CH_3OH on SnO_2. (f) CH_3OH on TiO_2.

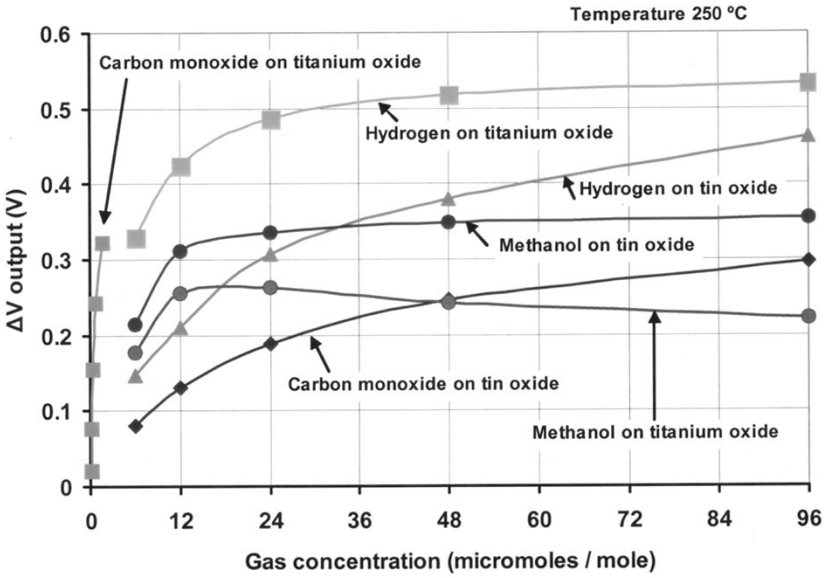

Fig. 15. Gas concentration versus ΔV output voltage.

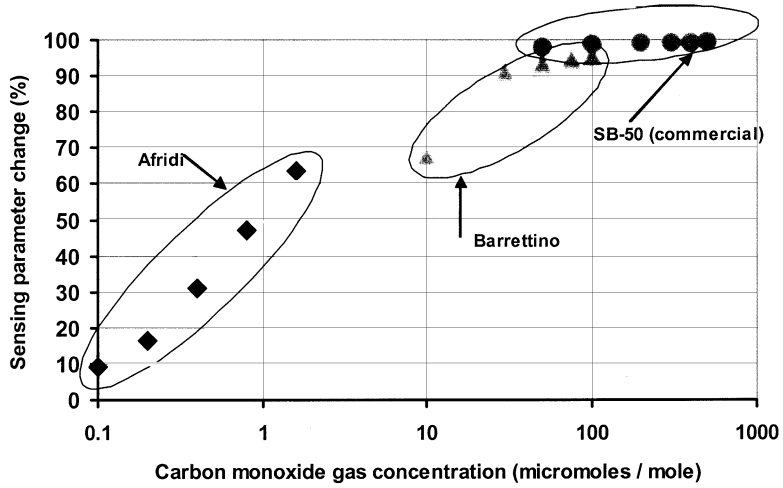

Fig. 16. Gas sensor response comparison.

bipolar transistors are suitable for driving heater elements of the microhotplate structures and MOSFETS are suitable for addressing the desired sensing film. An on-chip operational amplifier used for measuring the sensing film conductance is described, and measurements are given. The operational amplifier gives a robust output signal. Gas sensing operation is demonstrated for concentrations down to 100 nanomoles/mole.

The presented gas sensor system demonstrates that by using CMOS compatible post processing steps to realize microhotplate structures and integrated electronics, low-cost, robust sensor systems can be implemented on a common substrate. Other issues regarding packaging and sensor reliability will need to be addressed in future work before such systems can become commercially viable.

REFERENCES

[1] M. Gaitan, J. S. Suehle, R. E. Cavicchi, and S. Semancik, "Micro-hotplate devices and methods for their fabrication," U.S. Patent 5 464 966, Nov. 7, 1994.

[2] V. Demarne and A. Grisel, "An integrated low-power thin-film CO gas sensor on silicon," *Sens. Actuators*, vol. 13, pp. 301–313, 1988.

[3] M. Parameswaran, A. M. Robinson, D. L. Blackburn, M. Gaitan, and J. Geist, "Micromachined thermal radiation emitter from a commercial CMOS process," *IEEE Electron Device Lett.*, vol. 12, pp. 57–59, Feb. 1991.

[4] J. S. Suehle, R. E. Cavicchi, M. Gaitan, and S. Semancik, "Tin oxide gas sensor fabricated using CMOS micro-hotplates and in-situ processing," *IEEE Electron Device Lett.*, vol. 14, p. 118, Mar. 1993.

[5] D. Moser, O. Brand, and H. Baltes, "A CMOS compatible thermally excited silicon oxide beam resonator with aluminum mirror," in *Proc. Transducers '91*, pp. 547–550.

[6] J. Jaeggi, H. Baltes, and D. Moser, "Thermoelectric AC power sensor by CMOS technology," *IEEE Electron Device Lett.*, vol. 13, p. 366, July 1992.

[7] M. Y. Afridi, J. S. Suehle, M. E. Zaghloul, D. W. Berning, A. R. Hefner, S. Semancik, and R. E. Cavicchi, "A monolithic implementation of interface circuitry for CMOS compatible gas-sensor system," in *Proc. IEEE Int. Symp. Circuit and Systems*, May 2002, pp. II 732–735.

[8] N. H. Tea, V. Milanovic, C. Zincke, J. S. Suehle, M. Gaitan, M. E. Zaghloul, and J. Geist, "Hybrid postprocessing etching for CMOS compatible MEMS," *J. Microelectromech. Syst.*, vol. 6, pp. 363–372, Dec. 1997.

[9] P. K. Clifford and D. T. Tuma, "Characteristics of semiconductors gas sensors II. Transient response to temperature change," *Sens. Actuators*, vol. 3, pp. 255–281, 1982/83.

[10] C. J. Taylor and S. Semancik, "Use of microhotplate arrays as microdeposition substrates for materials exploration," *Chem. Mater.*, vol. 14, pp. 1671–1677, 2002.
[11] A. Hefner, D. Berning, D. Blackburn, C. Chapuy, and S. Bouche, "A high-speed thermal imaging system for semiconductor device analysis," in *Conf. Proc. 17th Annu. IEEE Semiconductor Thermal Measurement and Management Symp.*, Mar. 2001, pp. 43–49.
[12] M. Afridi, D. Berning, A. Hefner, J. Suehle, M. Zaghloul, E. Kelley, Z. Parrilla, and C. Ellenwood, "Transient heating study of microhotplates by using a high-speed thermal imaging system," in *Conf. Proc. 18th Annu. IEEE Semiconductor Thermal Measurement and Management Symp.*, Mar. 2002, pp. 92–98.
[13] R. J. Baker, H. W. Li, and D. E. Boyce, *CMOS Circuit Design, Layout, and Simulation*. Piscataway, NJ: IEEE Press, 1998, pp. 617–634.
[14] D. Barrettino, M. Graf, M. Zimmermann, A. Hierlemann, and H. Baltes, "A smart single-chip micro-hotplate-based chemical sensor system in CMOS-technology," in *Conference Proc. 2002 IEEE Int. Symp. Circuits and Systems*, May 2002, pp. II-157–160.

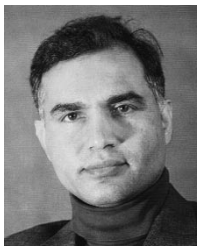

Muhammad Y. Afridi (M'97) was born in Lahore, Pakistan, in October 1960. He received the B.Sc. degree in electrical engineering from the University of Engineering and Technology, Lahore, Pakistan, in 1986 and the M.S. degree in computer science and the D.Sc. degree in electrical engineering from The George Washington University, Washington, DC, in 1994 and 2002, respectively.

He was awarded a Graduate Research Fellowship with the National Institute of Standars and Technology (NIST), Gaithersburg, MD, for the years 1997 through 2002. His areas of interest include analog and digital interface circuit design and fabrication for MEMS-based microsensors devices. He is currently working within a system-on-a-chip (SoC) project at NIST.

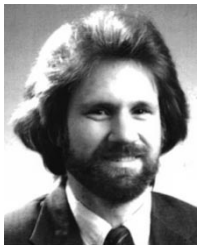

John S. Suehle (S'81–M'82–SM'95) received the B.S., M.S., and Ph.D. degrees in electrical engineering from the University of Maryland, College Park, in 1980, 1982, and 1988, respectively.

In 1981, he received a Graduate Research Fellowship with the National Institute of Standards and Technology (NIST), Gaithersburg, MD. Since 1982 he has been working in the Semiconductor Electronics Division at NIST where he is leader of the Advanced MOS Device Reliability and Characterization Project. His research activities include failure and wear-out mechanisms of semiconductor devices, radiation effects on microelectronic devices, microelectromechanical systems (MEMS), and molecular electronic devices. He has published over 100 technical papers or conference proceedings and holds 5 U.S. patents.

Dr. Suehle is a member of Eta Kappa Nu.

Mona E. Zaghloul (M'81–SM'85–F'96) received the M.A.Sc. degree in electrical engineering, the M.Math. degree in computer science and applied analysis, and the Ph.D. degree in electrical engineering from the University of Waterloo, Waterloo, ON, Canada, in 1970, 1971, and 1975, respectively.

Since 1989, she has been a Professor in the Electrical and Computer Engineering Department of The George Washington University, Washington, DC, and from 1994 to 1998, she was Chair of the Department. In addition, she directs the Institute of MEMS and VLSI Technology, George Washington University, which encompasses several interdisciplinary faculties and over a dozen graduate students with funding from NIST, DARPA, NASA, and the Navy. She has worked extensively in the general areas of circuits and systems, nonlinear systems, and microelectronic systems since 1975. She has published over 190 technical papers and reports in the areas of circuits and systems theory, nonlinear system theory, micromachining MEMS sensors design, and micro-electronic VLSI analog and digital circuits design, and has contributed to four books. Since 1984, she has worked as a faculty hire at the Semiconductor Devices Technology Division, National Institute of Standards and Technology (NIST).

Dr. Zaghloul is currently the Associate Editor for the IEEE SENSORS JOURNAL. She was an Associate Editor for the IEEE TRANSACTIONS ON CIRCUITS AND SYSTEMS I for neural networks from 1993 to 1995 and for the IEEE TRANSACTIONS ON CIRCUITS AND SYSTEMS PART II for sensors from 1999 to 2001. She was the Vice President of IEEE-CAS Technical Activities from 2000 to 2001.

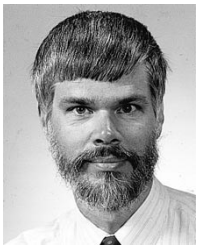

David W. Berning was born in Cincinnati, OH, in 1951. He received the B.S. degree in physics from the University of Maryland, College Park, in 1973.

He joined the National Bureau of Standards (now the National Institute of Standards and Technology) in 1974, where he remains today. Much of his career has focused on semiconductor device reliability, first using laser-scanning techniques to probe active devices, and later using electrical methods to explore safe operating area for power devices. He is currently involved in developing techniques for characterizing high-voltage, high-speed SiC power diodes and MOSFETs. He holds three U.S. patents in the area of audio amplifier design.

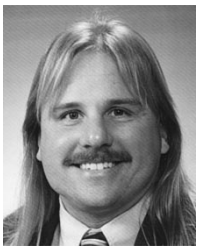

Allen R. Hefner (S'83–M'84–SM'93–F'01) was born in Washington, DC, on June 29, 1959. He received the B.S., M.S., and Ph.D. degrees in electrical engineering from the University of Maryland, College Park, in 1983, 1985, and 1987, respectively.

He joined the Semiconductor Electronics division of the National Institute of Standards and Technology (NIST), Gaithersburg, MD, in 1983. He is presently the Group Leader for the NIST Semiconductor Electronics Division's Device Technology Group. His research interests include characterization, modeling, and circuit utilization of power semiconductor devices and MEMS-based integrated sensor System-on-a-Chip technologies. He is the author of 60 publications in IEEE Transactions and Conference proceedings.

Dr. Hefner received a U.S. Department of Commerce Silver Metal Award in 1993 for his pioneering work in modeling advanced power semiconductor devices for electro-thermal circuit simulation. He is also the recipient of the 1996 NIST Applied Research Award for development and transfer of the IGBT model to circuit simulator software vendors and the recipient of an IEEE Industry Applications Society prize paper award. He has presented 30 invited seminars and was an instructor for the IEEE Power Electronic Specialist Conference tutorial course (1991 and 1993) and for the IEEE Industry Applications Society Meeting tutorial course (1994). He has served as a program committee member for the IEEE Power Electronics Specialist Conference (1991–1999) and the IEEE International Electron Devices Meeting (2001–2002), and as the Transactions Review Chairman for the IEEE Industry Applications Society Power Electronics Devices and Components Committee (1989–1997). He has also served as the IEEE Electron Device Society Standards Technical Committee Chairman (1996–2001) and is a member of the IEEE Electron Devices Society Power Devices and Integrated Circuits Technical Committee and the IEEE Power Electronic Society Technical Committee for Computers in Power Electronics.

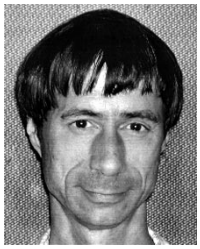

Richard E. Cavicchi received the B.S. degree in physics from the Massachusetts Institute of Technology, Cambridge, in 1980 and the Ph.D. degree in physics from Cornell University, Ithaca, NY, in 1987. His master's thesis focused on laser light scattering from colloidal crystals. His dissertation focused on electron tunneling in small metal particles at low temperatures.

He is a Physicist at the National Institute of Standards and Technology (NIST), Gaithersburg, MD. While a post-doctoral at AT&T Bell Laboratories (1986–1988), he investigated carrier transport in quantum well devices. He joined NIST in 1989, where he has worked in the area of chemical sensors. This work includes the surface characterization of sensor interfaces, studies of sensor materials, micromachined device design, and novel sensing strategies.

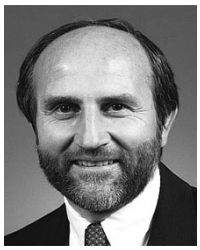

Steve Semancik received the B.S. degree in physics from Rensselaer Polytechnic Institute, Troy, NY, in 1974 and the Sc.M. and Ph.D. degrees in physics from Brown University, Providence, RI, during 1976 and 1980, respectively.

He was then awarded a National Research Council Postdoctoral Associateship to do experimental studies in the Surface Science Division at the National Institute of Standards and Technology (NIST), Gaithersburg, MD. In late 1982, he joined the Process Measurements Division at NIST as a Research Physicist and became Project Leader of NIST's program in solid state chemical sensing. His work has included research on oxide surfaces, thin-film growth, model catalytic systems, surface structural transitions, and the kinetics of fundamental surface reactions. His recent activities have been focused on developing improved materials for chemical sensing and combining active films with micromachined structures to realize advanced microsensor devices and operating modes. He is an author of approximately 100 papers and five patents.

Dr. Semancik is a Fellow of the American Vacuum Society.

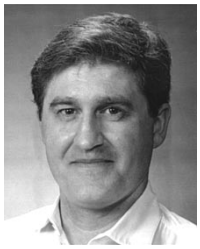

Christopher B. Montgomery was born in Hartford, CT, in September 1960.

He began his career as an Organosilane and Silicone Chemist in 1983 with Petrarch Systems, Inc. In 1994, he worked for SAIC developing self-assembled silane monomolecular layer protocols for hippocampal neuronal networks on patterned silane-modified surfaces. In 1997, he joined Commonwealth Scientific, Inc./Veeco Instruments, Inc. as a vacuum thin-films process engineer. In 2000, he joined the National Institutes of Standards and Technology, Gaithersburg, MD, and is currently a member of the Process Measurements Division of the Chemical Science and Technology Laboratory where he micromachines MEMS devices and prepares platforms for use as metaloxide gas sensors. In addition, he performs vacuum thin-films research for fabricating or modifying a variety of microelectromechanical devices.

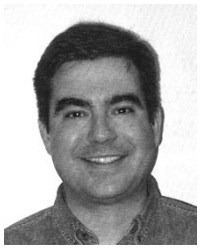

Charles Taylor received the B.A. degree in chemistry from Macalester College, St. Paul, MN, and the Ph.D. degree in chemistry from the University of Minnesota, Minneapolis, in 1999.

His graduate research focused on the role of precursor chemistry in the development of microstructure in CVD aluminum and titanium dioxide thin films. From 2000 to 2002, he was a National Research Council Postdoctoral Associate at the National Institute of Standards and Technology (NIST), Gaithersburg, MD. He is currently an Assistant Professor of chemistry at Pomona College, Claremont, CA. His current research interests are in the field of chemical sensing and microsensor design.